Journal of Power Sources 183 (2008) 381–387

Contents lists available at ScienceDirect

Journal of Power Sources

journal homepage: www.elsevier.com/locate/jpowsour

Current and potential distributions on positive plates with conductive Pb_3O_4 and $BaPbO_3$ in their formation and discharge

Yonglang Guo*, Huan Liu

College of Chemistry and Chemical Engineering, Fuzhou University, Fuzhou 350108, PR China

ARTICLE INFO

Article history:
Received 7 February 2008
Received in revised form 9 April 2008
Accepted 28 April 2008
Available online 14 May 2008

Keywords:
Conductive materials
Current and potential distributions
Formation
Lead-acid batteries
Positive plates

ABSTRACT

The positive plates with conductive materials, Pb_3O_4 and $BaPbO_3$, in automotive lead-acid batteries were investigated by measuring their current and potential distributions in the course of formation and discharge. It is found that these two conductive materials, especially Pb_3O_4, enhance the formation in the initial stage greatly and that they make the current and potential distributions more uniform. In the discharge, the addition of Pb_3O_4 increases the capacity of the positive plate, but it is unfavorable to the paste curing and causes poor contact between active mass (AM) particles so that the polarization increases greatly at 3 C discharge rate. The $BaPbO_3$ additive improves not only the formation but also the discharge performance because of its stability in acidic media and at high polarization. The violent charge at high polarization around the plates in the initial formation can lead to poor AM contact and high polarization resistance.

1. Introduction

Although the lead-acid batteries have been widely used in automotive, vehicle traction and other industry applications due to their low cost and high performance, there still exist many problems for positive plates, such as grid corrosion, active mass (AM) softening and low AM utilization [1,2]. These problems are closely related to the manufacturing technology of the positive plate and its paste formula [3]. The former includes the curing and the formation, etc. The latter is mainly composed of the lead powder, sulfuric acid and water. It is significant to use the AM additives of the positive plate to promote the formation and increase AM utilization [4–6].

The specific energy of lead-acid batteries is largely limited by the positive plate, whose performance is greatly affected by the formation [7]. As the porosity of the positive active mass (PAM) decreases in the formation, the transformation of the positive paste into PbO_2 becomes more difficult. It normally takes very long time, especially for the thick or tubular positive plate and the container formation of valve-regulated lead-acid (VRLA) batteries [8]. The formation of the positive plate depends on the cured paste composition, acid density of the formation electrolyte, charge current profile and electrolyte temperature [9–13]. The technology applied needs to obtain a high content of PbO_2 and an appropriate ratio of α-PbO_2 to β-PbO_2 in PAM, in order to ensure the initial capacity of the battery and its life [14].

The cured paste of the positive plate is composed of lead sulfate, lead oxide, tri- and tetra-basic lead sulfates (3BS and 4BS). Since they are very poor conductors or insulators, very high charge current density appears in the initial stage of the formation, which results in a very high polarization and violent gassing. In order to improve the conductivity and reduce the polarization, the addition of red lead (Pb_3O_4) to PAM has been widely used by many manufacturers [15–17]. Besides the thick or tubular positive plates of large lead-acid batteries and the container formation of VRLA batteries, recently Pb_3O_4 is also employed in the container formation technology of flooded automotive VRLA batteries with the thin plate cured at high temperature. Other conductive additives in the positive paste like $BaPbO_3$, Ti_4O_7 and graphite, etc. are also investigated [18–23]. They enhance the formation greatly in the early stage and increase the formation efficiency.

Although great efforts are made in the practical manufacture, there always exists difference in different parts of the same plate due to the plate dimension, grid design, paste mixing, pasting symmetry and formation, etc. [24,25]. This obviously affects the AM utilization as well as the performance of lead-acid batteries. Sunu and Burrows [26] predicted the potential and current distributions on the surface of the orthogonal grids according to each intersection and the conductivity of grid members. Calábek et al. [27,28] simulated the discharge of a positive–negative electrode pair and optimized the orthogonal grid design according to the current dis-

* Corresponding author. Tel.: +86 591 8789 2893; fax: +86 591 8807 3608.
E-mail address: yguo@fzu.edu.cn (Y. Guo).

0378-7753/$ – see front matter © 2008 Elsevier B.V. All rights reserved.
doi:10.1016/j.jpowsour.2008.04.092

tribution. Other simulation investigations include the current and potential distributions in the discharge of the flat, horizontal and spirally designed plates [29–31]. However, less work is done to measure the current and potential distributions of the practical plate. In our previous works, an in situ electrochemical scan technique has been established to study the current and potential distributions of various lead-acid battery plates and much information has been obtained about them in their formation and discharge [32,33]. In this paper, the effects of conductive substances, red lead and barium metaplumbate ($BaPO_3$), in the paste on the current and potential distributions in the positive plate formation and its discharge are studied.

2. Experimental

The commercial red lead was used and barium metaplumbate was prepared by calcining the mixture of red lead and barium carbonate with 1:1 molar ratio at 850 °C for 3 h in the air. The positive grids used were cast by multiple Pb–1.8%Sb alloy and were the rectangle design with the dimensions of 14.3 cm (W) × 13 cm (H) × 0.22 cm (T). The positive paste was composed of 1 kg lead powder, 0.7 g fibre, 20 g Pb_3O_4 or $BaPbO_3$ additive, sulfuric acid and distilled water. It contained 50 g H_2SO_4 per 1 kg lead powder and its apparent density was 4.2 g cm^{-3}. The pasted positive plate with 119 g paste was cured at 50–55 °C in 95–100% relative humidity for 24 h and was dried through reducing the relative humidity and elevating the temperature in 24 h. In order to eliminate the effects of the negative plate in the measurements, the pre-formed negative plates are used. Then one unformed positive plate and two formed negative plates were formed at 2.2 A in 1.05 g cm^{-3} H_2SO_4 (40–45 °C) for 22 h. The C_{20} capacity of the positive plate was 12 Ah.

To measure the current and potential distributions of the positive plate, an experimental set-up was described in detail in the previous work [24,25]. In short, the tested positive plate was placed between two formed negative plates. The container used had the internal dimensions of 14.5 cm (W) × 15 cm (H) × 8.4 cm (L). The distance between the positive and negative plates was about 3.8 cm. When the positive plate was formed or discharged, the IR voltage drop appeared in the electrolyte. Two $Hg/Hg_2SO_4/H_2SO_4$ (1.285 specific gravity) reference electrodes were used to measure the local IR drop in the electrolyte and the local potential on the positive plate. The measurement distance of the two reference electrode tips was 3 cm. The data of 162 points were obtained by scanning the three couples of reference electrodes from the bottom to top of the positive plate twice. The IR voltage drop and the electrode potentials were recorded by a HP 34970A Data Acquisition/Switch Unit connected to a PC. The charge–discharge processes was controlled by BT2000 Arbin Instruments.

3. Results and discussion

The synthesized $BaPbO_3$ was analyzed by X-ray diffractometer (XRD) and its three characteristic diffraction peaks appeared at 29.70° (relative intensity: 100%), 42.34° (18.3%) and 52.68° (31.5%), respectively. There are no diffraction peaks of other compounds. It indicates that the synthesized material is $BaPbO_3$.

To measure the local current density and potential, the test positive plate was divided into six channels. One scan measured three channels by moving three couples of reference electrodes from bottom to top of the plate, and the IR voltage drop in the electrolyte and the reference electrode potential close to the test plate were recorded per 0.5 cm height. So 162 points were measured in two scans and each point corresponded to 1.148 cm^2. The sum of 162 IR voltage drops, $\sum \Delta U$, was proportional to half of the total charge current, I, and each IR voltage drop, ΔU, was proportional to the local current in the area of 1.148 cm^2. Although great changes took place in the sulfuric acid concentration in the formation, the time needed in the measurements of 162 points was short and hence the electrolyte resistance, i.e. R value above, was supposed to be unchanged during the two scans. Therefore, the local current density, i, was calculated by the following expression

$$i = \frac{\Delta U \times I}{1.148 \times \sum \Delta U} \quad (1)$$

where I was equal to 1.1 A for 2.2 A formation current and 18 A for 36 A discharge current, respectively.

In the early stage of the formation, the high polarization and uneven current distribution appeared because of the poor conductivity of the paste. However, the polarization fell and the current distribution tended to be uniform with forming. After about 10 h formation, most of the paste was transformed into lead dioxide on the positive plate and the oxygen evolution was dominant. Then the current distribution became increasingly uniform. So Figs. 1 and 2 only show the current density distributions on three positive plates with and without conductive Pb_3O_4 and $BaPbO_3$ at 1 and 8 h formation, respectively. Its apparent current density is 5.92 mA cm^{-2} at 2.2 A. It is found that the current distribution is quite uneven on the three positive plates in Fig. 1, although the formation proceeds for 1 h. On the whole, the current density around the three plates is obviously higher than that in their middle. This is because only a little paste is transformed into conductive lead dioxide at this time and the big frame of the rectangle grid has higher conductivity. Although there have been many reports on the conductive additives or substances promoting the formation and used in the practical applications [16–23], Fig. 1 shows that the addition of Pb_3O_4 greatly improves the current distribution in the 3/4 regions of the positive plate except near the lug. $BaPbO_3$ additive in Fig. 1C1 only improves

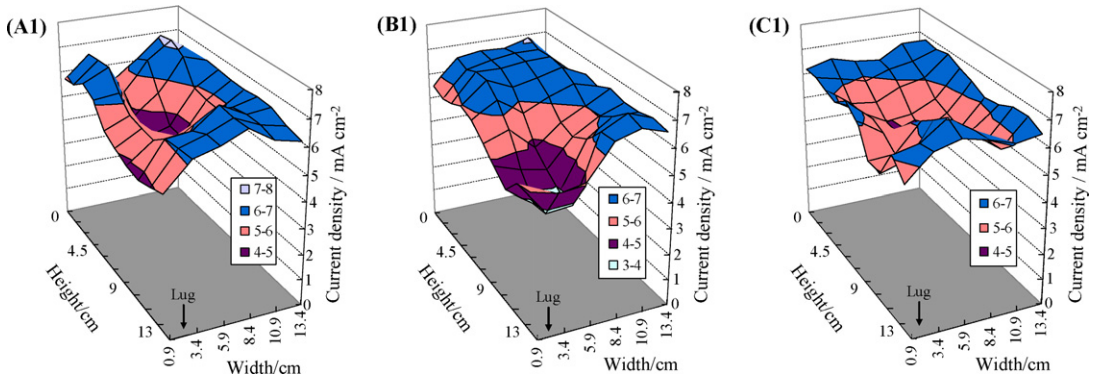

Fig. 1. The current density distributions on positive plates (A1) without conductive material and with (B1) Pb_3O_4 and (C1) $BaPbO_3$. Formation time: 1 h.

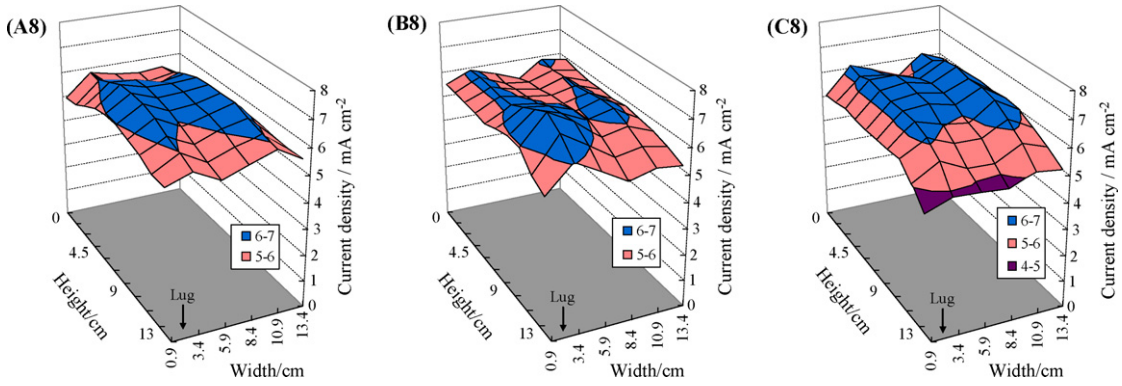

Fig. 2. The current density distributions on positive plates (A8) without conductive material and with (B8) Pb_3O_4 and (C8) $BaPbO_3$. Formation time: 8 h.

a little. It is well known that the Pb_3O_4 has good conductivity and is widely used as a component in the positive paste formula to enhance the formation. In Fig. 1B1, however, the current density near the lug of the positive plate is much lower than that in lower parts. This is different from the expected results that the highest current density should appear near the lug. This may be due to the uneven mixing and dispersal of Pb_3O_4 and the preferential spread of PbO_2 zone near conductive Pb_3O_4. In the practical manufacture, the Pb_3O_4 particles are large and are very difficult to disperse in the paste, which can be observed from the red color on the practical cured positive plates. At 8 h formation, Fig. 2 shows that the current distributions become relatively uniform on the three plates. The high current appears only where the current is low in the middle of three plates in Fig. 1. But the current in the upper part of the plate with $BaPbO_3$ additive drops more quickly as compared with the other two plates.

In order to compare the difference clearly among the three plates, Fig. 3 shows the evolution of the current distributions from the bottom to top in the middle parts of the three plates in their formation. The greatest difference of the current distributions occurs in the early stage of the formation and the distribution becomes increasingly uniform as the formation proceeds. At 1 h formation, the current density in the middle is much lower than that in the upper and lower parts of the plates (Fig. 3A). The difference between the highest and lowest current density reaches 2.48 mA cm^{-2} on the plate without conductive substances while it is only 1.57 and 1.77 mA cm^{-2} on the plate with conductive Pb_3O_4 and $BaPbO_3$, respectively. It is seen from Fig. 3A and B that the uniformity order of the current distributions on the three plates is Pb_3O_4 > $BaPbO_3$ > no conductive substance. At 8 h formation, their differences become very small. The current density in the upper and lower parts of the plates is a little lower than that in the middle where it is smaller in the early stage of the formation. There is hardly any change in the current distributions in the subsequent formation. At 22 h formation, the current density at the bottom increases a little while it drops at the top obviously, in comparison with the current density at 8 h formation. The falling of the current density in the upper parts in Fig. 3D is related to the high polarization in this region at the beginning of the formation, which will lead to high contact resistance between the AM particles.

Figs. 4 and 5 show the potential distributions on different positive plates at 1 and 8 h formation, respectively. At 1 h formation, the potential around the plate in Fig. 4A1 is obviously lower than that in the middle because of the good conductivity of the grid frame. And the lowest polarization appears in the upper parts of the plate. When $BaPbO_3$ was added to the paste, the average potential of the positive plate in Fig. 4C1 decreases by 4 mV and the potential in the upper parts falls a little more, but their potential distributions are almost the same. It indicates that the $BaPbO_3$ additive does not have much effect on the paste conductivity in the early stage of the formation. Fig. 4B1 shows that Pb_3O_4 reduces the polarization of the positive plate greatly. The average potential in the 3/4 regions decreases by 30 mV and the potential difference reaches about 37 mV in most parts of the plate in Fig. 4B1, compared with Fig. 4A1. It is clear that Pb_3O_4 has good conductivity and enhances

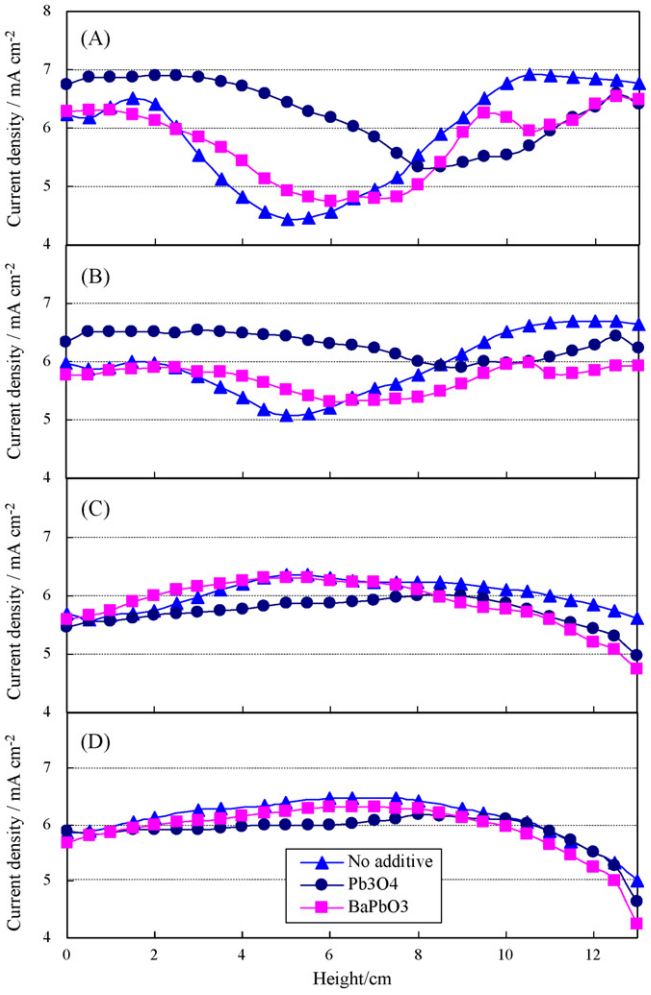

Fig. 3. The current density distributions in the middle parts (Channel 4) of positive plates with different conductive materials at different formation times. Formation time: (A) 1 h; (B) 2 h; (C) 8 h; (D) 22 h.

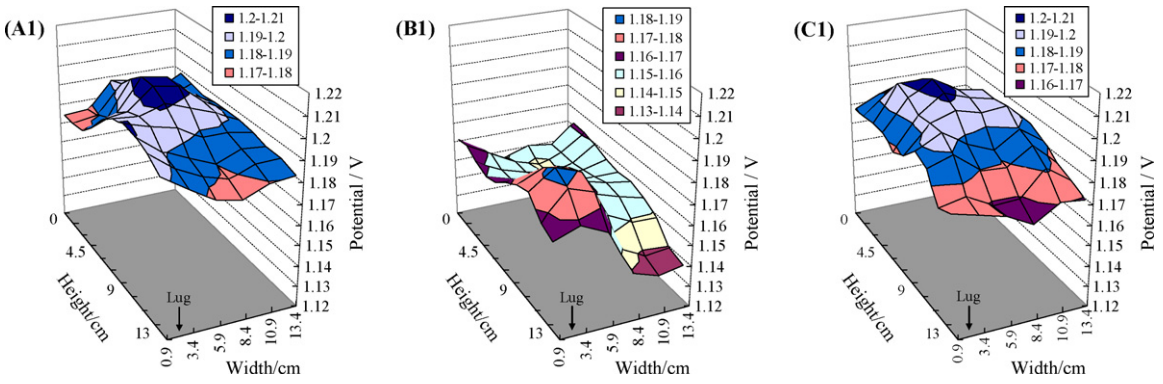

Fig. 4. The potential distributions on positive plates (A1) without conductive material and with (B1) Pb_3O_4 and (C1) $BaPbO_3$. Formation time: 1 h.

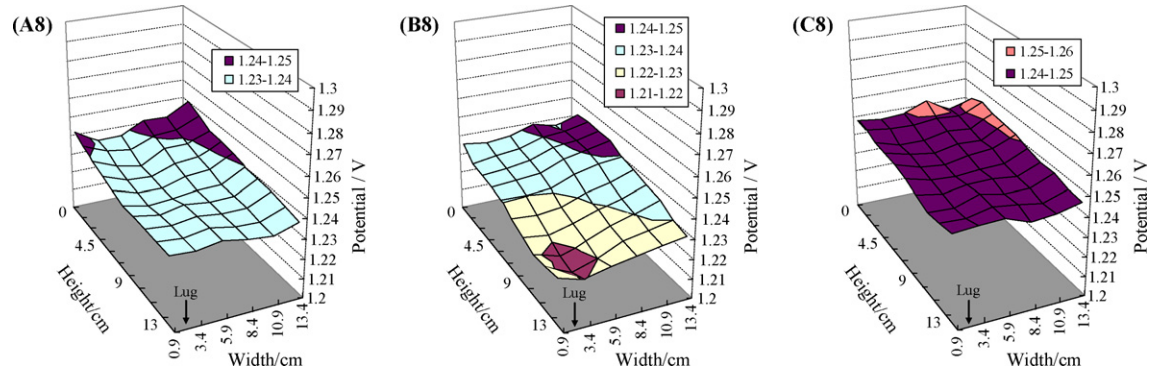

Fig. 5. The potential distributions on positive plates (A8) without conductive material and with (B8) Pb_3O_4 and (C8) $BaPbO_3$. Formation time: 8 h.

the formation greatly, which is in agreement with the action of the Pb_3O_4 in the practical application. However, an abnormal phenomenon appears in Fig. 4B1, that is, the polarization near the lug is not low but high. It is close to the data in Fig. 4A1. This may be due to the fact that the Pb_3O_4 particles are large and their dispersal is not uniform, which is often observed from red color distribution on the cured positive plate.

At 8 h formation, most parts of the positive paste are transformed into lead dioxide and the remainder is difficult to be formed so that the polarization increases greatly in Fig. 5. At this time, the potential distribution has become relatively uniform. And the polarization in the upper parts of the plate is only a little lower than that in the lower parts. The low polarization near the lug in Fig. 5B8 is related to the delayed formation in Fig. 4B1. As reported [21], the conductive additives can play an important role in the early stage of the formation, yet their action becomes inconspicuous as the conductive network of lead dioxide is established. In comparison, the average potential in Fig. 5C8 is a little higher, but the potential changes only within 14 mV among the three plates with different conductive materials.

Fig. 6 shows the evolution of the average potential obtained by 162 measurement points on three positive plates. During the initial 2 h formation, the potential of the three positive plates drops quickly and reaches the minimum. Then it increases gradually and tends to be stable after 10 h formation. At the beginning of the formation, the paste composed of basic lead sulfates and lead oxide has very high resistance and the formation first starts from the neighborhood of grid bar. As the PbO_2 zones are formed and advance into the paste, the current density decreases and so does the polarization [34]. The addition of Pb_3O_4 and $BaPbO_3$ increases the paste conductivity and hence reduces the polarization of the plates greatly. Fig. 6 shows that the action of Pb_3O_4 is more evident. At 2 h formation, the average potentials are 1.159, 1.140 and 1.148 V for the positive plates without any additive, with Pb_3O_4 and $BaPbO_3$, respectively. Therefore, the conductive materials can diminish the polarization of the positive plates and enhance their formation greatly.

In order to know the effects of the AM conductive materials on the positive plate performance, the positive plates which had been formed and dried were discharged at the 3 C rate (36 A) in the H_2SO_4 solution of 1.28 specific gravity. The amount of each recharge is about 125% discharge capacity. The measurements of the current and potential distributions on the positive plate were conducted in the same container as in the formation, in which the test positive

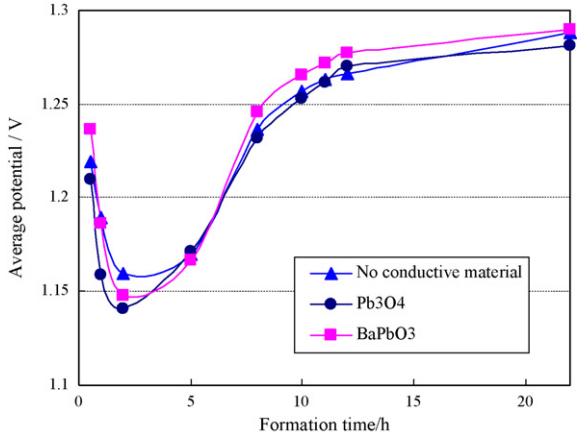

Fig. 6. Evolution of the average potentials on positive plates with and without conductive materials during the formation.

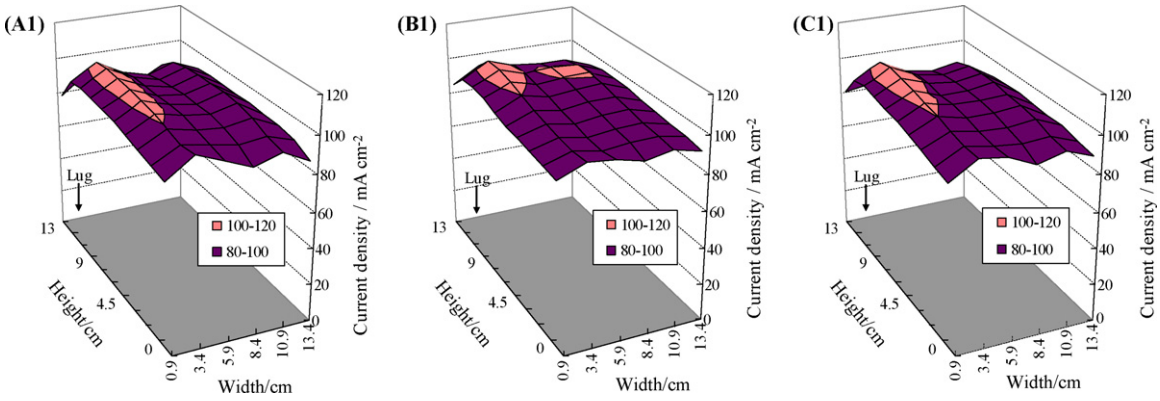

Fig. 7. The current density distributions on positive plates (A1) without conductive material and with (B1) Pb_3O_4 and (C1) $BaPbO_3$ at 3 C discharge rate. Discharge time: 1 min.

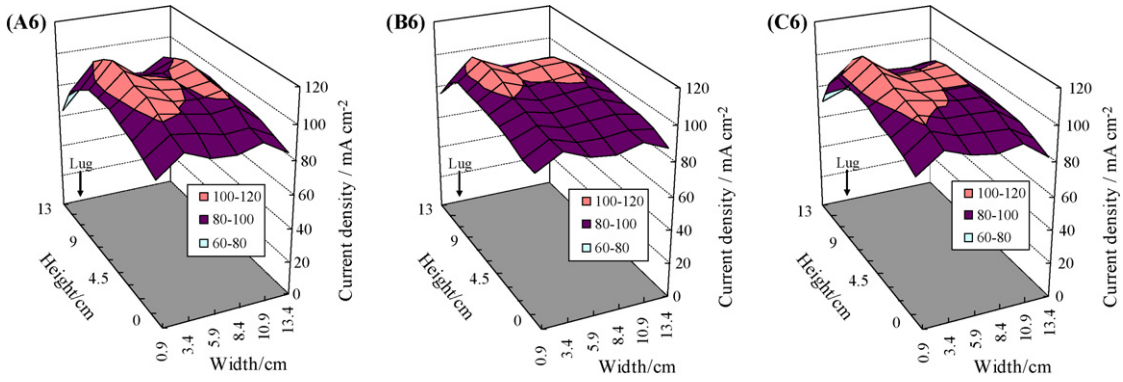

Fig. 8. The current density distributions on positive plates (A6) without conductive material and with (B6) Pb_3O_4 and (C6) $BaPbO_3$ at 3 C discharge rate. Discharge time: 6 min.

plate was put between two negative plates [25]. Figs. 7 and 8 show the current density distributions on the three positive plates at 3 C discharge rate at 1 and 6 min, respectively. It is noticed that their lug positions are different from those in Figs. 1 and 2, thus a better view is presented. At 1 min in Fig. 7, the current distributions of the three positive plates with and without conductive materials are similar and relatively uniform. The current density increases gradually with the height of the plate, but it decreases close at the top of the plate. At the end of the discharge in Fig. 8, their distributions become a little uneven. The current density falls in the upper and lower parts of the plates while it rises in the middle. In order to compare the three plates more clearly, Fig. 9 shows the change of their current density distributions from the bottom to top in the middle of the positive plates. In the initial discharge in Fig. 9A, the current density distributions of the three plates are the same in the lower part but different in the upper part. And the positive plate with Pb_3O_4 has higher current density. With discharging, the current density rises in the middle while it falls at the bottom and top of the plates in Fig. 9A, but it drops faster at the top. Its change trend on the plate with $BaPbO_3$ is very similar to that on the plate without conductive materials. However, the current density on the plate with Pb_3O_4 drops more quickly in the lower part. It means that the Pb_3O_4 may be unfavorable to the electrochemical performance of the plate although it enhances its formation.

Figs. 10 and 11 show the potential distributions on the three positive plates at 3 C discharge rate at 1 and 6 min, respectively. At 1 min in Fig. 10, their potential distributions are similar. The potential decreases gradually from the upper to lower parts of the plates due to the high discharge current and the grid resistance. The maximum potential difference reaches about 100 mV. But at

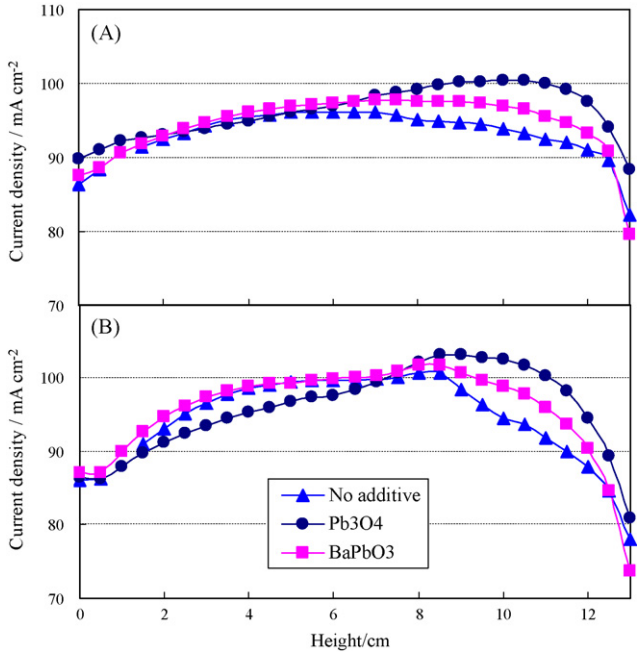

Fig. 9. The current density distributions in the middle parts (Channel 4) of positive plates with different conductive materials at 3 C discharge rate. Discharge time: (A) 1 min; (B) 6 min.

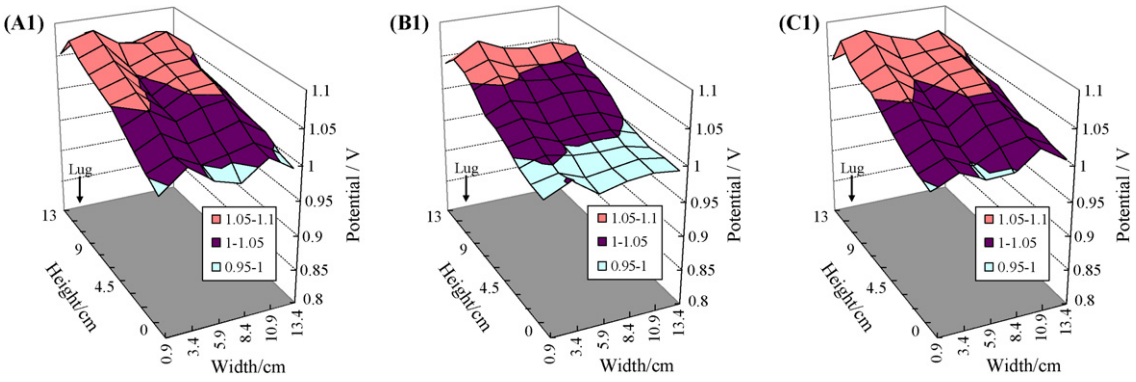

Fig. 10. The potential distributions on positive plates (A1) without conductive material and with (B1) Pb_3O_4 and (C1) $BaPbO_3$ at 3 C discharge rate. Discharge time: 1 min.

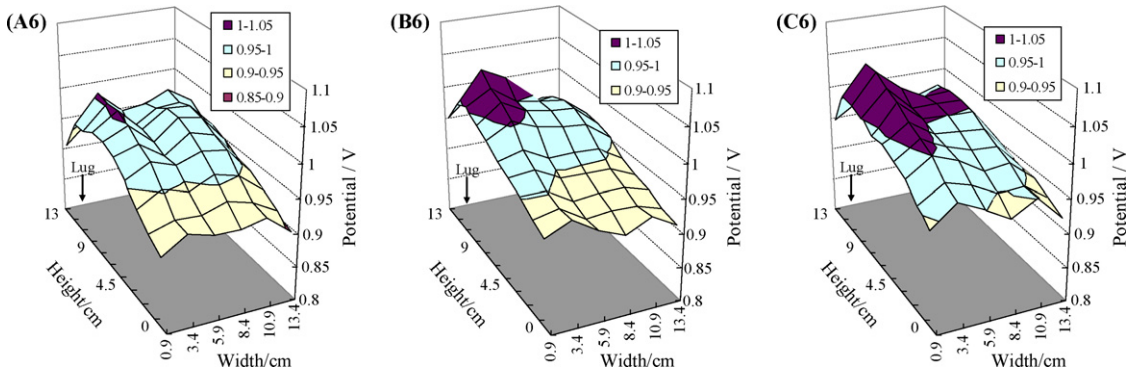

Fig. 11. The potential distributions on positive plates (A6) without conductive material and with (B6) Pb_3O_4 and (C6) $BaPbO_3$ at 3 C discharge rate. Discharge time: 6 min.

the top, the polarization becomes high, where the current density is low in Fig. 7. It means that the high polarization appears at the top of the plates, which is closely related to the high current in these regions in the initial formation (Fig. 3A and B). In comparison with Fig. 10A1 (no conductive materials), the $BaPbO_3$ additive does not affect the potential distribution (Fig. 10C1), while Pb_3O_4 makes the average polarization increase by 21 mV. As the discharge proceeds, the potential of positive plates decreases gradually and the larger potential falling occurs in the upper parts. At the end of the discharge in Fig. 11, the polarization of the three plates increases greatly and their potential distributions become more uneven. Apart from the polarization rising of the overall plate, the potential in the upper parts of the three plates drops more quickly, compared with Fig. 10. And at this time, the potential distribution on the plate with Pb_3O_4 (Fig. 11B6) is similar to that on the plate without conductive materials (Fig. 11A6). But the plate with $BaPbO_3$ additive has lower potential polarization in Fig. 11C6. It is obvious that $BaPbO_3$ has good conductivity and plays an important role in the latter discharge. To further understand the effects of conductive materials, the evolution of the average potentials on the three plates at 3 C discharge rate is shown in Fig. 12. Pb_3O_4 makes the polarization increase while $BaPbO_3$ reduces the polarization of the positive plate obviously during discharging due to its good conductivity and its stability. However, the potential of the positive plate without conductive materials drops quickly as the discharge proceeds. It indicates that the conductive $BaPbO_3$ improve the discharge performance of the positive plates greatly. Although the addition of Pb_3O_4 to the paste enhances the formation, it is transformed into PbO_2 in the formation, whose conductivity is the same as the PAM. In this case, Pb_3O_4 can increase the capacity of the positive plate, but it may affect the paste curing and recrystallization. This makes the contact between the AM particles poor and then the resistance of the plate increases, which can affect the battery life.

In order to obtain the resistance distribution, the open circuit potential of the fully charged positive plate was measured and it was 1.156 V in the H_2SO_4 solution of 1.28 specific gravity. When the positive plate is discharged, the polarization resistance is defined by the ratio of the electrode polarization to the current density. Fig. 13 shows the polarization resistance distributions on the three plates at the end of the discharge. Their distributions are similar and the polarization resistance is the lowest in the middle while it becomes very high around the plates. It is different from the

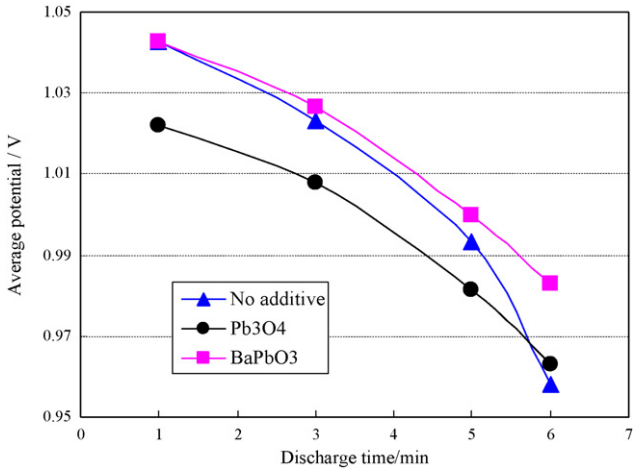

Fig. 12. Evolution of the average potential on three positive plates with and without conductive materials at 3 C discharge rate. Discharge time: 1 min.

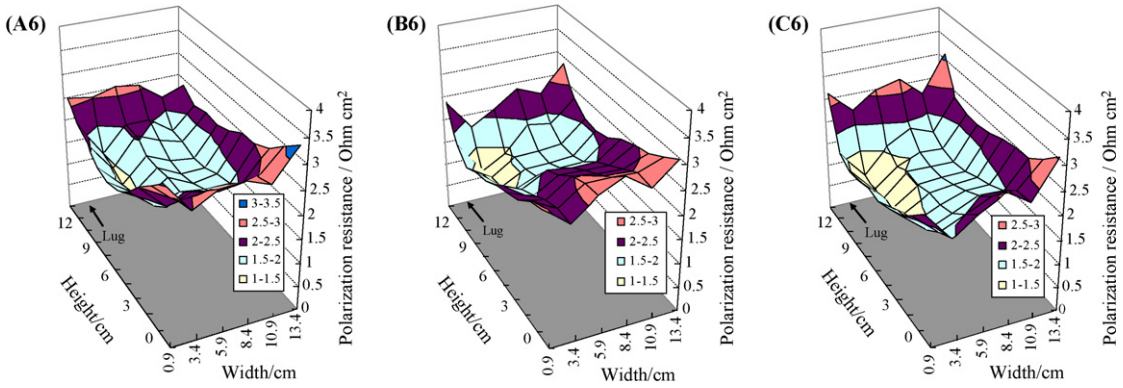

Fig. 13. The polarization resistance distributions on positive plates (A6) without conductive material and with (B6) Pb_3O_4 and (C6) $BaPbO_3$ at 3 C discharge rate. Discharge time: 6 min.

expected results that the lower polarization resistance is located near the grid frame with higher conductivity. It is related to the high polarization and high current density appearing around the plates in the initial formation (Figs. 1 and 4). This violent charge at the high polarization near the grid frame leads to poor contact between AM particles and thus the polarization resistance increases greatly. It can also be seen that the current distribution becomes more uneven at the end of the formation in Fig. 3D. The overcharge makes the current density at the top of the three plates drop obviously. In the whole discharge of the three plates in Fig. 9, the lowest current density appears at the top of three plates. Therefore, the current profile in the formation and the conductive materials in the paste can affect the performance of the positive plate greatly.

4. Conclusions

In this work, the effects of the conductive materials, Pb_3O_4 and $BaPbO_3$, in the positive plate pastes on the formation and the discharge performance were investigated by measuring the current and potential distributions. The formation of the positive plate begins more easily from the grid frame with good conductivity. Both Pb_3O_4 and $BaPbO_3$ enhance the formation in the initial stage (within 3–4 h) greatly, especially Pb_3O_4, which reduces the polarization significantly. The presence of these conductive materials also makes the current and potential distributions more uniform in the initial formation. However, they do not affect the latter formation much. At 3 C discharge rate, the current density is the highest in the middle of the positive plates and it is low in the upper and lower parts. And with discharging it drops obviously at the bottom and top. Pb_3O_4 can increase the capacity of the positive plate. But it makes the paste curing and the contact between AM particles poor, which results in the higher polarization resistance. So it is unnecessary to use high Pb_3O_4 content in the paste if its amount is enough to enhance the formation. Although $BaPbO_3$ is not as effective as Pb_3O_4 in enhancing formation, it has high stability in acidic media and at high polarization while Pb_3O_4 is transformed into PbO_2 after the formation. Therefore, $BaPbO_3$ can improve the performance of the positive plate greatly at a high discharge rate due to its good conductivity. The violent charge at the high polarization near the grid frame with better conductivity at the beginning of the formation can lead to poor AM contact and high polarization resistance.

Acknowledgements

The authors are grateful to NSFC (No. 20373037) in China and NSFC (No. E0510006) in Fujian Province for financial support for this work.

References

[1] D. Pavlov, G. Petkova, J. Electrochem. Soc. 149 (2002) A644–A654.
[2] R.J. Ball, R. Kurian, R. Evans, R. Stevens, J. Power Sources 109 (2002) 189.
[3] W.H. Kao, J. Electrochem. Soc. 143 (1996) 2841.
[4] K. McGregor, J. Power Sources 59 (1996) 31.
[5] P.T. Moseley, J. Power Sources 64 (1997) 47.
[6] P.W. Appel, D.B. Edwards, J. Power Sources 55 (1995) 81.
[7] T.C. Dayton, D.B. Edwards, J. Power Sources 85 (2000) 137.
[8] J.E. Manders, L.T. Lam, K. Peters, R.D. Prengaman, E.M. Valeriote, J. Power Sources 59 (1996) 199.
[9] D. Pavlov, G. Papazov, J. Electrochem. Soc. 127 (1980) 2104.
[10] Z. Takehara, K. Kanamura, J. Electrochem. Soc. 134 (1987) 13.
[11] A.T. Kuhn, J.M. Stevenson, J. Power Sources 10 (1983) 389.
[12] F. Steffens, J. Power Sources 31 (1990) 233.
[13] I. Dreier, F. Saez, P. Scharf, R. Wagner, J. Power Sources 85 (2000) 117.
[14] J.E. Manders, N. Bui, D.W.H. Lambert, J. Navarette, R.F. Nelson, E.M. Valeriote, J. Power Sources 73 (1998) 152.
[15] D.P. Boden, J. Power Sources 73 (1998) 56.
[16] J. Wang, S. Zhong, H.K. Liu, S.X. Dou, J. Power Sources 113 (2003) 371.
[17] E.E. Ferg, P. Loyson, A. Poorun, J. Power Sources 155 (2006) 428.
[18] K.R. Bullock, B.K. Mahato, W.J. Wruck, J. Electrochem. Soc. 138 (1991) 3545.
[19] D. Pavlov, N. Kapkov, J. Electrochem. Soc. 137 (1990) 16–21.
[20] S.V. Baker, P.T. Moseley, A.D. Turner, J. Power Sources 27 (1989) 127.
[21] W.-H. Kao, P. Patel, S.L. Haberichter, J. Electrochem. Soc. 144 (1997) 1907.
[22] W.-H. Kao, S.L. Haberichter, P. Patel, J. Electrochem. Soc. 141 (1994) 3300.
[23] W.-H. Kao, K.R. Bullock, J. Electrochem. Soc. 139 (1992) L41.
[24] Y. Guo, Y. Li, G. Zhang, H. Zhang, J. Garche, J. Power Sources 124 (2003) 271.
[25] Y. Guo, X. Zhou, M. Huang, H. Liu, J. Power Sources 157 (2006) 571.
[26] W.G. Sunu, B.W. Burrows, J. Electrochem. Soc. 128 (1981) 1405;
W.G. Sunu, B.W. Burrows, J. Electrochem. Soc. 129 (1982) 688;
W.G. Sunu, B.W. Burrows, J. Electrochem. Soc. 131 (1984) 1.
[27] M. Calábek, K. Micka, P. Bača, P. Křivák, J. Power Sources 85 (2000) 145.
[28] P. Král, P. Křivák, P. Bača, M. Calábek, K. Micka, J. Power Sources 105 (2002) 35.
[29] Z. Mao, R.E. White, B. Jay, J. Electrochem. Soc. 138 (1991) 1615.
[30] J.N. Harb, R.M. LaFollette, J. Electrochem. Soc. 146 (1999) 809.
[31] Y. Morimoto, Y. Ohya, K. Abe, T. Yoshida, H. Morimoto, J. Electrochem. Soc. 135 (1988) 293.
[32] Y. Guo, W. Li, L. Zhao, J. Power Sources 116 (2003) 193.
[33] Y. Guo, J. Appl. Electrochem. 36 (2006) 363.
[34] D. Pavlov, G. Papazov, V. Iliev, J. Electrochem. Soc. 119 (1972) 8.